

# Direct Photopatterning of Electrochromic Polymers

Jacob Jensen, Aubrey L. Dyer,\* D. Eric Shen, Frederik C. Krebs, and John R. Reynolds

Propylenedioxythiophene (ProDOT) polymers are synthesized using an oxidative polymerization route that results in methacrylate substituted poly(ProDOTs) having a  $M_n$  of 10–20 kDa wherein the methacrylate functionality constitutes from 6 to 60% of the total monomer units. Solutions of these polymers show excellent film forming abilities, with thin films prepared using both spray-casting and spin-coating. These polymers are demonstrated to crosslink upon UV irradiation at 350 nm, in the presence of an appropriate photoinitiator, to render the films insoluble to common organic solvents. Electrochemical, spectroelectrochemical, and colorimetric analyses of the crosslinked polymer films are performed to establish that they retain the same electrochromic qualities as the parent polymers with no detriment to the observed properties. To demonstrate applicability for multi-film processing and patterning, photolithographic patterning is shown, as is desired for fully solution processed and patterned devices.

case of cationic dispersions with anionic polymers such as poly(styrene sulfonate)), which limits their applicability as full solution processability and patterning is desired for most device applications.

Alkyl and alkoxy substituted poly(propylenedioxythiophene)s (PProDOTs) are electrochromic conducting polymers that have excellent film forming abilities, which allow for a wide range of processing methods from solution.<sup>[10]</sup> Their relative ease and scale-up of synthesis make them ideal candidates for future electrochromic devices (ECDs). As films of PProDOTs are mechanically formable, they can be coated onto flexible substrates for use in a variety of flexible devices and displays.<sup>[6,14]</sup> We have recently shown that it is indeed possible to exploit these mechanical advantages by

## 1. Introduction

Electrochromic materials are promising for a variety of applications that span dynamic tinting windows and mirrors, color-changing displays, smart cards, and e-paper.<sup>[1]</sup> Electrochromic compounds constitute a group of chemical species and may be categorized by their solubility in different redox states<sup>[2]</sup> or by their chemical origin as either inorganic or organic.<sup>[3,4]</sup> Of the organic compounds having electrochromic properties, conjugated polymers (CP) are ideal candidates for printable large area displays, windows, mirrors and e-paper.<sup>[2,5–8]</sup> The synthetic flexibility in designing CPs is one of their merits and band-gap engineering has allowed color tuning of electrochromic polymers (ECPs). Just as important is the ability to make organic conducting polymers processable from organic, and in some cases, aqueous solutions.<sup>[9–13]</sup> While conjugated polymers such as poly(pyrrole)s, poly(aniline)s and poly(thiophene)s have been subject to intense investigation for their electrochromic properties,<sup>[1]</sup> a majority of those studies involve use of film preparation methods such as electrochemical polymerization (in the case of polypyrrole and polythiophene) and spin-casting (in the

using roll coating processes to develop electrochromic devices that rely on PProDOTs as the active electrochrome.<sup>[15]</sup> By use of PProDOTs, and ProDOT monomer units in combination with various other heterocycles and aryl units, the full color palette, desired for non-emissive displays, is now accessible.<sup>[16]</sup> Further research in ECPs should now focus on the processing of these materials to allow development into commercially viable applications. As such, understanding the electrochromic properties and advances in process development of PProDOTs have been a focus since ProDOTs were investigated as effective electrochromic polymers more than a decade ago.<sup>[17,18]</sup>

By taking advantage of the C2 symmetry in the ProDOT structure it is possible to functionalize the central bridging carbon atom twice while preserving the regiosymmetry of the monomer, and by extension, affording regioregular polymers. Functionalization at the bridging carbon affords two main advantages—improved electrochromic properties and solubility. It has been shown that this substitution gives rise to a less compact morphology, thereby allowing faster incorporation of counterions and faster switching rates.<sup>[9,18–20]</sup> The advantage of solution processable polymers cannot be understated and by appending various alkyl and alkoxy chains to the ProDOT monomer, spray processable polymers (namely PProDOT-(CH<sub>2</sub>OEtHx)<sub>2</sub>) with a transmittance contrast ( $\Delta\%$ T) approaching 80% were synthesized and devices fabricated.<sup>[9,21]</sup> In further advancing the processability of PProDOTs, ester functionalities have been incorporated that, after conversion to the corresponding salts, allow for processing from more environmentally benign solvents such as alcohols and water. These carboxylate substituted PProDOTs permit a short post-processing acid treatment yielding solvent resistant films.<sup>[22]</sup> The possibility of such orthogonal processing steps is advantageous in device fabrication.<sup>[20,23]</sup>

J. Jensen, Prof. F. C. Krebs  
Department of Energy Conversion and Storage  
Technical University of Denmark  
Frederiksborgvej 399, DK-4000 Roskilde, Denmark  
Dr. A. L. Dyer, Dr. D. E. Shen, Prof. J. R. Reynolds  
School of Chemistry and Biochemistry  
and School of Materials Science and Engineering  
Georgia Institute of Technology  
Atlanta, GA 30332, USA  
E-mail: aubrey.dyer@chemistry.gatech.edu



DOI: 10.1002/adfm.201203005

In addition to introducing processability through synthetic methods, there is the possibility of utilizing functionalities that allow for photolithographic patterning of CPs, a method commonly utilized in the semiconductor industry. Several methods of photolithographic patterning exist,<sup>[24–26]</sup> with the two main approaches employed being: Chemically Amplified Photolithography (CAP) and Non Chemically Amplified Photolithography (NCAP). The former relies on photochemical reactions that do not occur in the resist material, but rather triggers a response, upon irradiation, that induces a solubility change in the resist material. For polythiophenes this has been exploited with the use of thermally cleavable tetrahydropyranyl functionalities: upon exposure to a photogenerated acid, the deprotection temperature decreases and consequently the polymer becomes insoluble.<sup>[27]</sup> By employing CAP procedures, it is possible to avoid likely photobleaching of the thiophene backbone, that would lead to altering of the polymer optical properties, as the amplifier molecule absorbs the radiation during the liberation of the amplifying species (e.g. the acid in the above example). A NCAP approach, which has also been explored in relation to patterning of polythiophenes, is a method of photo-induced crosslinking.<sup>[26]</sup> In general, however, the irradiation source used in the direct procedure approach (laser, UV lamp, etc) generates free radicals, consequently damaging the thiophene ring by causing irreversible photobleaching, rendering the photoresist useless as an electroactive component.<sup>[28–31]</sup> This has, in some cases, been solved by attaching acrylate or methacrylate groups to the alkyloxy bridge of the thiophene ring.<sup>[33]</sup> By incorporation of a photoinitiator to absorb the radiation and appending C=C bonds to crosslink, it is possible to use lower doses of UV light, thereby sparing the thiophene ring.<sup>[32,33]</sup> An elegant way of preventing photooxidation of the parent thiophene ring was presented by Sotzing et al.<sup>[34]</sup> whereby, relying on crosslinking of methacrylate groups, the authors employ a precursor polymer that is already crosslinked prior to oxidative polymerization of the thiophene rings, allowing them to avoid harsh radiation procedures that have the potential of damaging the polymer backbone.

To achieve more than just academic value, the patterning of conducting polymers should be simple and avoid tedious post-processing steps such as etching, peeling of solid layers, etc. Conventional photolithography requires multiple steps and, while each step in itself is not complicated, the use of direct photopatterning to generate negative tones is facile and complementary to large scale manufacturing procedures. Depending on the usage of the electrochromic film, several coating methods are available and include spray-casting, slot-die coating, screen printing, and others.<sup>[35]</sup> In this report, we utilize drop-casting, spin-coating and spray-coating. While drop-casting was exclusively utilized for electrochemistry measurements and spin-coating reserved for solubility demonstrations, the technique utilized for the majority of this work was airbrush spraying. All of the above techniques are preferred for lab scale experiments, but if one desires to manufacture electrochromic displays on a larger scale, it is necessary to employ line-coating procedures, of which roll coating is advantageous and requires that the substrate to be coated is flexible. Here, it is helpful to turn to the various coating methods utilized in the extensive research surrounding organic and polymeric solar

cells, including the recent demonstration of the manufacturing of roll coated organic solar cells by one of our groups.<sup>[36]</sup>

Of the many roll coating techniques available, we have recently shown that electrochromic devices can be made by utilizing slot-die coating onto flexible substrates.<sup>[15,37]</sup> In this context, we report here a complementary method that will allow extension of the zero- and one-dimensional coating techniques previously demonstrated. Direct photopatterning of slot-die coated electrochromic films will transform this fast and reliable coating technique into a two dimensional method, which is traditionally associated with contact printing techniques such as flat bed screen printing, rotary screen printing, flexographic printing, gravure printing<sup>[38]</sup> and, to some extent, ink jet printing.<sup>[39]</sup>

However, compared to traditional photoresists, the photoresists used in electrochromic devices must preserve the electronic and optical properties of the materials. A simplified example of direct photopatterning, as demonstrated in this report, is depicted in **Figure 1**, wherein a solution processable polymer is cast onto a transparent conductive electrode (typically ITO/glass or ITO/plastic). This is followed by application of a photomask and irradiation (step A - Figure 1). The irradiation initiates crosslinking within the exposed areas of the polymer film. After irradiation, the mask is removed and the non-crosslinked (i.e., non irradiated) areas of the film are dissolved, leaving behind a negative image of the pattern (step B-Figure 1). Finally the electrochromic film is submerged in an appropriate electrolyte and electrochemically switched between the different oxidation states (step C-Figure 1).

In this paper, we report on the synthesis of a series of methacrylate substituted PProDOTs where the relative content of methacrylate functionality is varied. By varying the relative amounts of alkyl substituted-ProDOT and methacrylate substituted-ProDOT units, it was possible to synthesize random

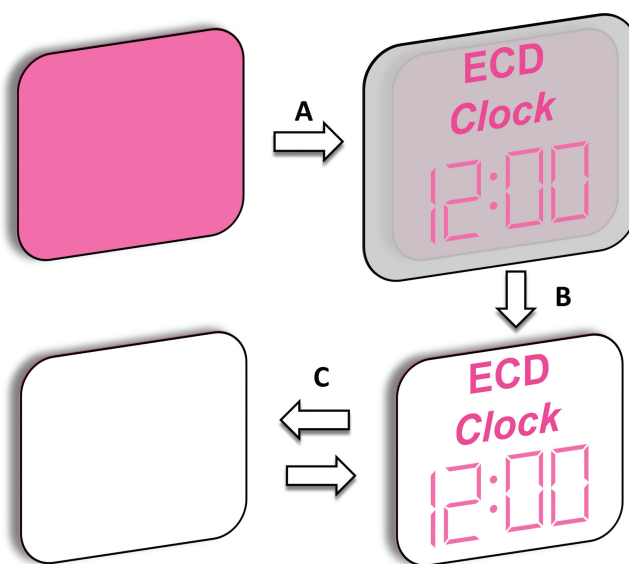
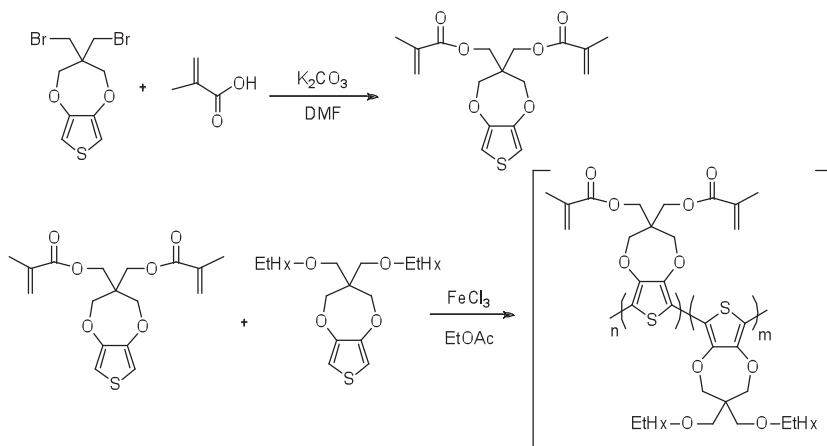


**Figure 1.** Principles of direct ECP photopatterning, starting from a conducting surface coated with ECP. A) Application of a photomask and irradiation. B) Dissolution of non-irradiated polymer. C) Electrochromic switching of crosslinked polymer.



**Scheme 1.** Synthetic route to bis-methacrylate containing comonomer and copolymers.

copolymers containing from 6% to 60% of bis-methacrylate monomers (e.g. copolymer 30 contains 30% bis-methacrylate monomer). The straightforward synthesis route leads to a set of polymers prepared via an oxidative polymerization route with number average molecular weights ( $M_n$ ) between 10 and 20 kDa that are highly soluble in common organic solvents. Utilizing photo-crosslinking results in thin polymer films that are rendered insoluble in common organic solvents, allowing patterning of electrochromic polymer thin films that switch between a highly colored and near colorless transmissive state. Most importantly, we demonstrate that photo-crosslinking of the polymers is possible with conservation of the electrochromic properties such that redox potentials, color, optical properties, contrast, and switching speeds are retained.

## 2. Results and Discussion

### 2.1. Synthesis

**Scheme 1** shows the synthetic route to the bis-methacrylate ProDOT-poly(3,4-dihydro-2H-thieno[3,4-b][1,4]dioxepine-3,3-diyl)bis(methylene)bis(2-methylacrylate), starting from available 3,3-bis(bromomethyl)-3,4-dihydro-2H-thieno[3,4-b][1,4]dioxepine. The starting material was reacted with methacrylic acid under basic conditions in dry DMF affording the bis-methacrylate thiophene, **1**, after purification by dry column vacuum chromatography (DCVC).<sup>[40]</sup>

**Table 1.** Polymer composition and molecular weight estimation by GPC.

Monomer 1 in reaction	Monomer 1 in polymer	Yield	$M_n$ [Da]	$M_w$ [Da]	PDI
10%	6%	36%	10500	22000	2
20%	12%	50%	15700	33500	2.1
50%	30%	31%	16900	31700	1.9
80%	60%	30%	7300 <sup>a)</sup>	15400	2.1

<sup>a)</sup>Crosslinking of the polymer was observed during analysis, which might cause a lower  $M_n$  to be detected.

By varying the amounts of the two monomers, we synthesized random copolymers containing from 6 to 60% (see **Table 1**) of the bis-methacrylate monomer by use of oxidative polymerization with ferric chloride in ethyl acetate. This method afforded copolymers in reasonable yields (30–50%) and with molecular weights ranging from 10 to 20 kDa. Compared to homopolymers of the bis-ethylhexyl monomers, which yield an  $M_n$  of 35 kDa when prepared under the same conditions, we believe that the acrylate groups impose steric hindrance during the polymerization resulting in lower  $M_n$  values. The composition of the copolymers was determined by FT-IR and  $^1\text{H}$  NMR. The  $^1\text{H}$ -NMR spectra of homopolymer (herein referred to as ECP-magenta) (A) and the copolymers containing various amounts of the bis-methacrylate monomer (B–E) are

found in the Supporting Information (Figure S1). The difference between the homopolymer of ECP-magenta and the copolymers is the peak at 1.97 ppm (methacrylate  $\text{CH}_3$ ) and the two peaks at 6.14 and 5.61 ppm (C=C protons) indicated by arrows. The increase in intensity of these peaks, in proceeding from A to E, is a consequence of a higher content of bis-methacrylate monomer in the copolymer, which was determined by integration to be from 6–60%. On comparison of the incorporated bis-methacrylate content in the copolymers to the percent of the bis-methacrylate utilized in the reaction mixture, it is noted that this polymerization favors incorporation of the bis-ethylhexyl monomer. We were able to estimate that the bis-methacrylate content of the copolymer to be consistently 60% of that in the reaction mixture, except for the highest content where it is 75% (column 1 and 2 in **Table 1**).

The FT-IR absorption spectrum of the copolymer containing 6% bis-methacrylate substituted monomer (copolymer 6) is shown in **Figure 2** and that for the bis-methacrylate monomer

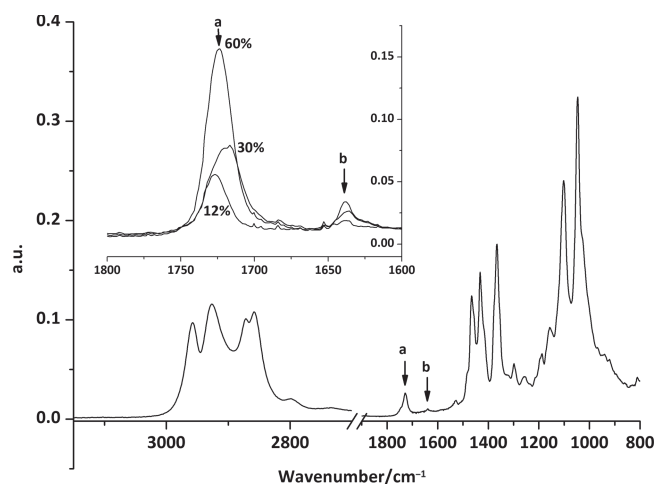


**Figure 2.** FT-IR of the bis-methacrylate copolymer A/Absorption spectra of the 6% copolymer (the 1800–1600  $\text{cm}^{-1}$  region for 12%, 30%, and 60% is shown in the inset). The arrows marked a and b indicate the C=O and C=C stretch respectively.

is available in the Supporting Information (Figure S2) for reference. In the latter, the band at  $3103\text{ cm}^{-1}$  is assigned to the C–H stretch on the 2- and 5-positions on the thiophene ring of the monomer and the band at  $2974\text{ cm}^{-1}$  is the methyl C–H stretch. The 2- and 5- C–H stretch from the thiophene monomer is not present in the polymer spectra (compare Supporting Information Figure S2 to Figure 2 and Supporting Information Figure S3), which indicates polymerization. Of particular interest is the intense sharp band at  $1712\text{ cm}^{-1}$  from the C=O stretch of the ester and the less intense band at  $1643\text{ cm}^{-1}$  from the C=C stretch in the acrylate (marked a and b respectively in Figure 2). These bands do not occur in IR spectra of the homopolymer ECP-magenta and confirms that the desired copolymer was synthesized. Preservation of the C=C stretches confirm that the acrylate groups are intact after the oxidative polymerization. The band at  $2974\text{ cm}^{-1}$  originating from the C–H stretch in the methyl group of the methacrylate does not show in Figure 2, as this region is populated by signals from various aliphatic groups. In the spectrum of the 100% bis-methacrylate homopolymer this band is visible. However, as the homopolymer was completely insoluble in common organic solvents it was considered not useful from a practical point of view (see Supporting Information Figure S3). The inset in Figure 2 shows the increasing absorption of the C=O and C=C bands as a result of increasing the bis-methacrylate monomer content in the feed. As the intensity of absorption bands is directly proportional to the content of the group resonating at that wavelength, the FT-IR and NMR data presented support each other satisfactorily.

## 2.2. Coating

To perform electrochemical measurements, thin films of the polymers were prepared by drop-casting the polymer solutions onto platinum button electrodes. While this is an often-used method of thin film formation for electrochemical measurements on small area electrodes, it should be noted that drop-casting is not well-suited for large area processing of polymer films as issues arise from inhomogeneous film drying and lack of control over dry film thickness. To prepare polymer films on larger area substrates for solubility studies, spin-coating was employed. This casting method is highly reproducible, affording films equivalent in thickness, density and morphology.<sup>[41]</sup> However, it should be noted that we did encounter inhomogeneous films when the methacrylate content of the copolymers was 60%. We ascribe this to a higher surface tension of the bis-methacrylate resulting in de-wetting (the acrylate functionality is more polar compared to the saturated alkyl functional groups). This issue was circumvented by switching the processing solvent for this particular polymer, allowing the formation of visually homogeneous films as detailed in the experimental section. To demonstrate a more practical method for large area processing, we employed airbrush spray-casting and utilized these films for spectroelectrochemical measurements and for the patterned electrochromic films. This method of preparing films of processable electrochromic polymers has been demonstrated to be ideal to produce electrochromic films with an open morphology that is believed to enhance optical

contrasts and switching speeds.<sup>[42]</sup> Details regarding solution compositions and photoinitiators used in crosslinking are found in the experimental methods section.

## 2.3. Crosslinking

In order to avoid photooxidation of the electrochromic polymer films, we used as mild conditions as possible in terms of irradiance and temperature exposure. This was addressed using several approaches: employing azobisisobutyronitrile (AIBN) as a photoinitiator and incorporation of a high degree of polymerizable acrylate sites. In regards to the first approach, AIBN was found to be a reliable photoinitiator and is soluble in the organic solvents used in formulating the polymer solutions. AIBN is a well-known azo-radical initiator that decomposes upon irradiation at wavelengths of 300–360 nm, yielding the 2-cyanoprop-2-yl radicals responsible for initiating the polymerization of the methacrylate groups. An additional product of the reaction is gaseous nitrogen, which is expected to evaporate from the polymer film with no observable damage due to nitrogen diffusion.

Another strategy to decrease the irradiance necessary for crosslinking was successfully realized by employing polymers containing a high degree of polymerizable acrylate sites. This was done by synthesizing bis-methacrylate monomers. As described in the introduction, the aliphatic groups in the 2-position on the ProDOT propylene bridge play a key role in controlling solubility and processability of these polymers, and by substituting the ethylhexyl groups with methacrylates, the solubility of the resulting polymers could be compromised. Indeed, an insoluble polymer was observed when the bis-methacrylate homopolymer was synthesized. However, by synthesizing copolymers comprising both monomers (see Scheme 1), it was possible to tune the solubility of the polymer, such that high quality films retaining full electrochromic properties could be cast, and subsequently crosslinked. This was accomplished by having the crosslinkable groups on the polymer backbone (as opposed to end groups). The resulting  $M_n$  ensured the favorable qualities of the polymers (saturated colors, processability, high film quality, etc.) without sacrificing the degree of crosslinking.

To monitor the crosslinking process, FT-IR spectroscopy was performed whereby thin polymer films were spin-cast onto freshly pressed KBr pellets and transmission spectra recorded after irradiation of the films at regular intervals. Figure 3 shows the results for copolymer 30, where depletion of the acrylate double bonds can be seen as the decrease of the band at  $1643\text{ cm}^{-1}$  upon irradiation. What is also observed is no change in the other bands present (especially the band at  $1712\text{ cm}^{-1}$  originating from the ester functionality), which demonstrates that the crosslinking proceeds exclusively through the carbon-carbon double bonds of the acrylate, without disrupting the ester functionality nor the ProDOT backbone. It can be seen from the time progression shown in Figure 3 that the majority of the crosslinking occurs within the first 240 seconds of irradiation. It should be noted that even upon longer exposures, the small peak at  $1643\text{ cm}^{-1}$  is not fully depleted. While the exposed surface of the polymer film is relatively uniform, the underlying structure is not due to the KBr pellet, on which the film is cast,



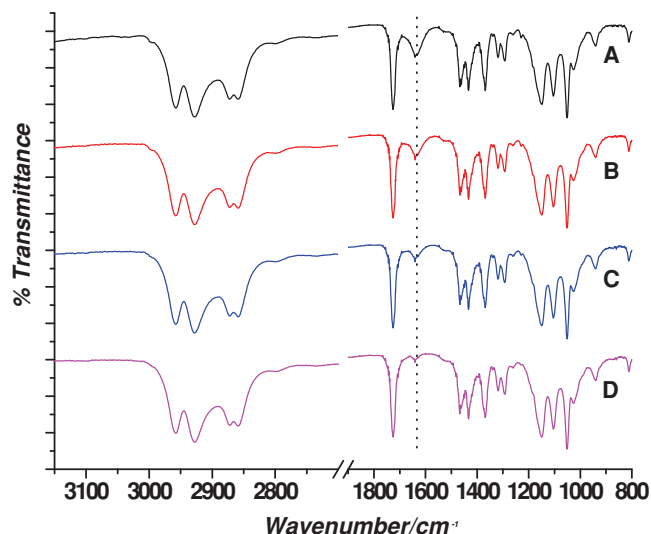


**Figure 3.** IR transmission spectra of the 30% copolymer during irradiation. A) 0 s, B) 60 s, C) 240 s, D) 960 s.

not being a flat surface, causing non-uniformity in crosslinking through the thickness of the polymer film.

In order to assess the effect of crosslinking on solubility in toluene, polymer solutions of the various copolymers were cast onto ITO-coated glass (as described in the Experimental Section), and irradiated. They were then submerged in a solution of stirring toluene at room temperature for 1 min and allowed to dry. Following this, the transmission profiles of the films were measured and compared to spectra obtained prior to toluene treatment as shown in **Figure 4**.

To be of interest in electrochromic devices, the optical properties of the conjugated polymer should be retained after irradiation and crosslinking, as is demonstrated in **Figure 4**. The as-cast films are shown as the traces labeled as 'A' for the 30% copolymer (left) and 60% copolymer (right). The films were then irradiated for 600 seconds and immersed in stirred toluene for 60 s to remove any polymer not rendered insoluble by crosslinking. The spectra labeled as 'B' are of the films after this treatment. It can be seen that a relatively small fraction

of material was removed in the 30% copolymer film as indicated by a 20% increase in transmission at the  $\lambda_{\max}$ . For the 60% copolymer, even less material was removed as shown in the spectra on the right by a minimal 2% increase in transmission. A difference in extent of crosslinking is expected as the 60% copolymer has twice as many acrylate functional groups to allow for reaction upon irradiation, allowing for a higher extent of crosslinking. When films of the alkoxy homopolymer (ECP-Magenta) were subjected to the same conditions, the films fully dissolved in under 10 s. Likewise, the 6% and 12% copolymers exhibited a slight decrease of solubility on crosslinking, compared to the alkoxy homopolymer and were not further studied. In further work, it is expected that the extent of crosslinking can be increased in the copolymers containing 6% to 30% acrylate functionality by varying the relative concentration of the diacrylate additive or utilizing an additive with a longer chain or increased functionality (e.g., tetraethyleneglycoldiacrylate or pentaerythritol triacrylate).

It should be noted that there is a small extent of crosslinking occurring under normal laboratory conditions as shown in the spectra labeled as 'C' that are of spin cast films of the acrylate functionalized polymer films not irradiated in the photoreactor, followed by immersion in stirring toluene. This is attributed to a combination of emission of UV radiation from the fluorescent room lighting and thermal initiation of the AIBN. As the focus of this work is the synthesis of newly functionalized electrochromic polymers that allow photoinduced crosslinking and their characterizations in regards to preserving electrochromic properties post-processing, it is understood that further work remains in regards to optimization of the photoinitiator and crosslinking conditions. For example, AIBN is known to decompose thermally at 65 °C. While it was found stable to handling at standard atmospheric conditions, the relatively low decomposition temperature does pose a challenge upon selective irradiation as the substrate material and/or photomask may reach temperatures approaching the AIBN decomposition temperature, resulting in crosslinking non-irradiated areas of the film. Furthermore, future work should include use of appropriate UV light filters, as is typically utilized in photopatterning-intensive laboratories, to selectively block UV emission from typical laboratory fluorescent lamps as the irradiation from room lighting can initiate crosslinking.

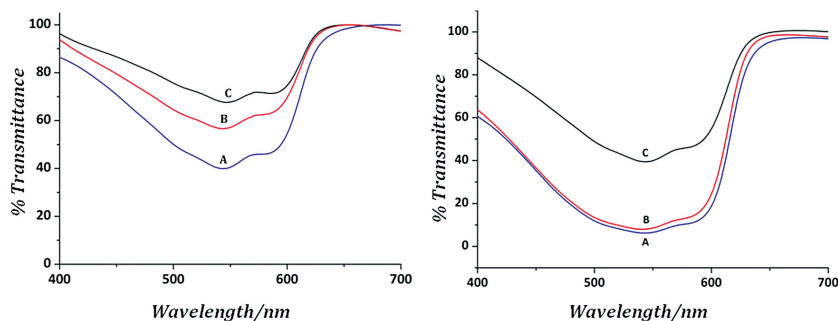


**Figure 4.** Transmission profiles for spin-cast polymer films after various treatments. The left hand graph was normalized to compensate for reflections in the glass substrate (resulting in transmittance above 100%). The spectra on the left are of copolymer 30 and on the right of copolymer 60. The A curves show the transmittance profile of the pristine films, while the B curves are of films cured for 600 s and then immersed in toluene for 60 s, and the C curves are of the uncured film after dissolution in stirring toluene for 60 s.

## 2.4. Electrochemistry

The electrochemical behavior of the polymer films was investigated by use of cyclic voltammetry. Of particular interest were differences in redox activity that may result from replacement of the ethylhexyloxy groups at the C2 carbon of the propylene bridge with methacrylate groups, and upon crosslinking of polymer films. **Figure 5A** provides the CV scans for the 50th cycle for both copolymer 30 and 60 with that of the homopolymer ECP-Magenta presented in the Supporting Information (Figure S4). While there are several similarities in the current–voltage profiles

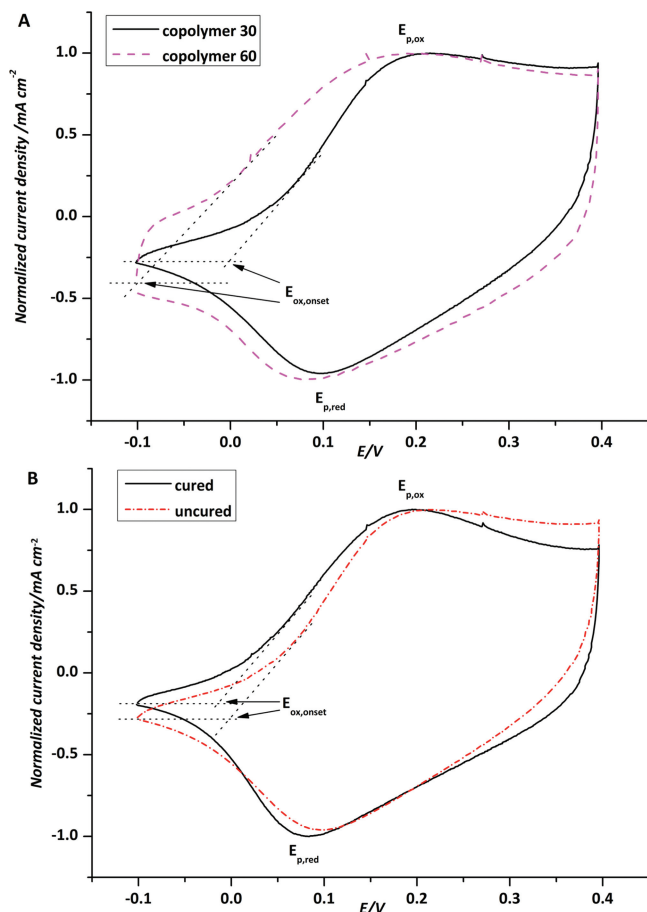


**Figure 5.** Cyclic voltammetry analysis of ECP films. A) CV of copolymer 30 (solid line) and copolymer 60 (dotted line). B) CV before (dotted line) and after (solid line) 600 s of irradiation (crosslinking) of copolymer 30. Normalized current density is displayed to counterbalance any effects of inhomogeneity of film thickness drop-casting might have. All reported potentials are relative to  $\text{Ag}/\text{Ag}^+$ .

between these three polymers, there are several differences that can be ascribed to the acrylate functionality. The redox switching windows were similar for all three polymers with the onset of oxidation,  $E_{\text{ox}}$ , observed to be 0 V and −0.1 V for the copolymers 30 and 60 respectively, while  $E_{\text{ox}}$  was 0.1 V for ECP-Magenta. A consequence of the acrylate functionality is a broader redox process and higher level of charging current during cycling due to the acrylate functionality that can lightly crosslink under ambient conditions. The broad redox process for the acrylate-functionalized polymers is similar to that seen for the first CV scan of the alkyloxy homopolymer in Supporting Information Figure S5. The homopolymer has been shown to undergo an ‘electrochemical annealing’ process on the first cycle, resulting in a reordering of the polymer chains to adopt a more ordered conformation (this can also be observed in the spectral data discussed later), which can be seen by the sharper redox peaks for the second (and subsequent) CV scans. However, in the acrylate-functionalized polymers, a low level of crosslinking causes the polymer chains to lock in their conformation and not reorder on redox switching. This semi-locked conformation can also lead

to a larger component of the current resulting from diffusional-dependent double-layer charging as the solvated counter ions are more restricted in their ability to diffuse through the polymer film. This is further supported by the higher background charging current observed in copolymer 60 than in copolymer 30 as shown in Figure 5A, where copolymer 60 has a higher density of acrylate functionality and, hence, a larger amount of ambient crosslinking occurring. We can exclude any differences between the copolymers and homopolymer being due to electrochemical crosslinking as there is an absence of additional redox peaks within the potential window scanned and therefore conclude that no electrochemical polymerization of the acrylate functionality occurs in addition to no additional insolubilization observed. This indicates that the acrylate functionality is stable within the potential window scanned.

In utilizing crosslinkable functionalities, the retention of electroactivity in the polymer films after photo-induced crosslinking, is essential. In Figure 5B below, we present a CV scan of a pristine copolymer 30 film overlaid with that of a polymer film after photo-induced crosslinking after 600 s of irradiation, as detailed in the experimental section. This demonstrates that the polymer electroactivity is preserved in the crosslinked film as there is essentially no change in the redox peaks indicating that there are no detrimental side reactions on UV exposure.

## 2.5. Spectroelectrochemistry and Colorimetry

Films were spray-cast from toluene solutions as detailed in the experimental section and spectroelectrochemistry was performed *in situ* by measuring the absorbance spectrum at a desired applied potential with the potential stepped in increasing increments of 50 mV. Figure 6 shows the absorbance spectra of films of copolymer 30 and homopolymer ECP-Magenta in the fully neutral and fully oxidized states (the

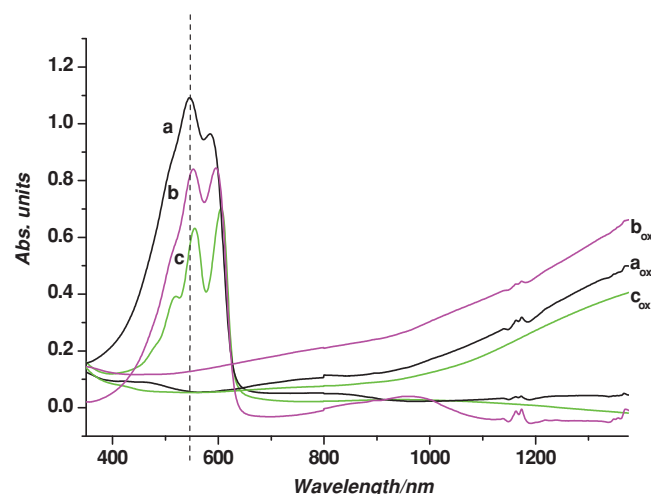


**Figure 6.** Spectroelectrochemistry of methacrylate copolymers and ECP-Magenta homopolymer. The graphs a and a(ox) show the absorbance of copolymer 30 at 0 V and 0.4 V, respectively, prior to crosslinking. Graph b and b(ox) are copolymer 30 at 0 V and 0.4 V after irradiation for 600 s (crosslinking). Graphs c and c(ox) show homopolymer ECP-Magenta.

full spectroelectrochemical series is provided as Supporting Information, Figure S6). By comparing spectra a, b, and c, the onsets of absorption are observed to occur at similar wavelengths, with only minor differences between the spectra in regards to relative peak intensities. The copolymer before and after crosslinking (spectra a and b, respectively), show similar absorption profiles in the neutral state with a  $\lambda_{\text{max}}$  centered at 548 nm and an absorption onset at 620 nm. The homopolymer ECP-Magenta exhibits a slightly red-shifted spectra in addition to a higher degree of vibronic coupling, which is typical of this polymer.<sup>[9]</sup> This is not unexpected in light of the electrochemical data, given that the homopolymer has the conformational freedom to reorder on electrochemical cycling to form a highly ordered structure, resulting in the vibronic coupling. However, the acrylate polymer, with a low level of crosslinking occurring under ambient conditions, is partially locked in conformation and is not able to order, resulting in a broader absorption profile in the neutral state. On oxidation, the absorbance in the visible region decreases due to depletion of the  $\pi$ - $\pi^*$  transition while absorptions at longer wavelengths begin to appear due to the introduction of lower energy electronic transitions (polarons and bipolarons). Upon full oxidation, the polymer has little absorption in the visible region as nearly all of the absorption is now occurring in the near infrared, with little tailing into the visible region as is also seen for the alkoxy-substituted homopolymer. This indicates that there is no loss of electrochromic switching on UV exposure and the copolymer retains a high level of optical contrast before and after crosslinking.

To quantitatively describe the color of the electrochromic films as perceived by the human eye, colorimetry was employed using a Minolta colorimeter and a standard background illumination as detailed in the experimental section. The 1976 CIE LAB ( $L^*a^*b^*$ ) method was utilized to represent colors measured *in situ* at different applied potentials, shown in Figure 7A. As the potential applied to the film was progressively stepped from fully neutralizing to fully oxidizing values, the  $a^*$ ,  $b^*$  values decreased from 46, -32 when colored (indicating a color with a blue-red component as expected for a magenta film) at -0.1 V to -1, -1 when fully bleached (indicating a highly achromatic film) at the applied potential of 0.35 V. These values are very similar to those previously reported for the ECP-Magenta homopolymer.

The lightness, or  $L^*$ , is a measure of the weighted response of the eye to light intensity variations (whereas transmittance is a linear response of a photodetector) and was simultaneously measured as shown in Figure 7B as a function of applied voltage. In the fully neutralized state at -0.1 V, the polymer is in a colored, absorptive state, transitioning to a near colorless, high lightness state between 0.1 and 0.2 V until fully oxidized when the  $L^*$  maximizes at 93. This is also seen in the inset photographs. Similarly with the  $a^*$  and  $b^*$  values there is negligible difference in the  $L^*$  values between the films before and after photo-crosslinking, except for a slightly higher  $L^*$  value in the neutral state, which can be ascribed to a slight loss of non-crosslinked material in the film after crosslinking and rinsing, as was also observed in the spectra. This minimal difference of the  $L^*a^*b^*$  values measured between the pristine and crosslinked films supports the analysis that crosslinking does not affect the optical and color properties of the polymer films in either the neutral or oxidized states.

### 3. Patterning

To realize the full potential of electrochromic conjugated polymers, the development of practical processing and patterning methods is of major importance. To demonstrate this, we have previously shown that large area devices incorporating electrochromic polymers and semi-solid ionic gels can be achieved by coating onto flexible substrates using commonly used coating techniques such as slot-die coating. When considering these practical printing and processing methods, the ability to directly pattern a material is highly desirable; especially fine, detailed patterns. However, with the zero- and one-dimensional methods previously mentioned, direct patterning is not possible. The ability to print a soluble material using roll-to-roll methods, followed by photolithographic patterning will allow for large area processing with small feature patterning as desired for display applications. To that end, we preliminarily demonstrate the use of photolithographic patterning using the 30% copolymer as shown in Figure 8. In this method, we have spray-cast a thin polymer film from toluene, followed by 600 s of irradiation through a shadow mask as shown in Figure 8B. The irradiated

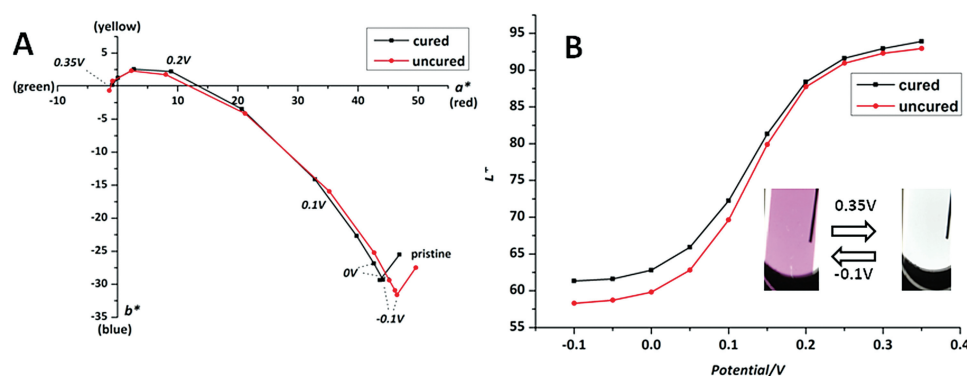


**Figure 7.** Colorimetry measurements of cured and uncured copolymer 30. A) Development of  $a^*$  and  $b^*$  at increasing potentials. B) Lightness ( $L^*$ ) as a function of applied potential. Inset photographs show the film switched at the oxidized and neutral state. All reported potentials are relative to  $\text{Ag}/\text{Ag}^+$ .

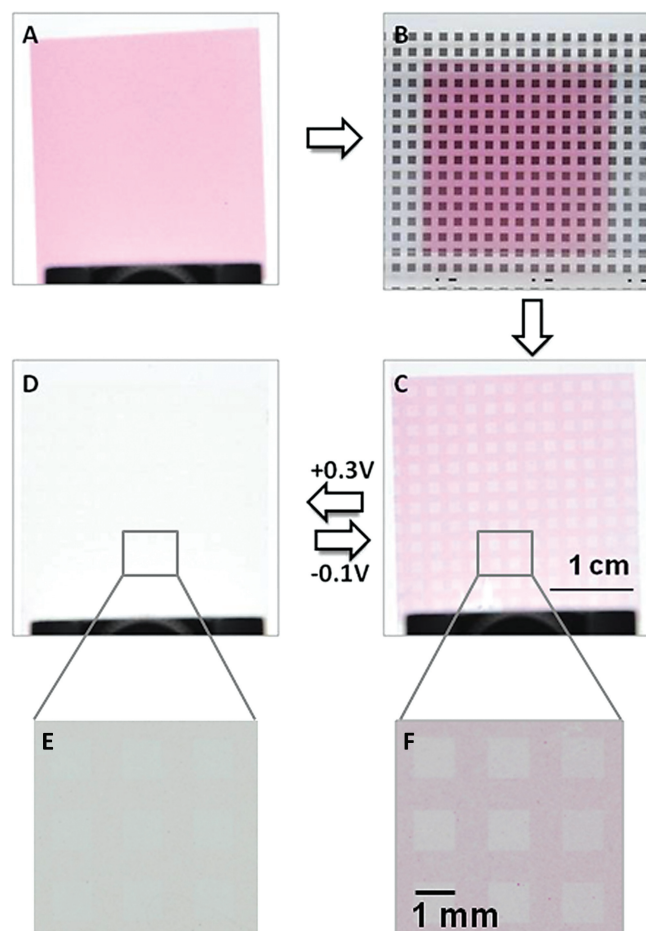


**Figure 8.** Direct photopatterning of methacrylate-substituted ECP-Magenta. A) An ECP-coated ITO/glass substrate. B) Application of a photomask followed by 600 s of irradiation. C) Film in the neutral state following dissolution of non-irradiated polymer in toluene and repeated switching. D) Film in the oxidized state following repeated switching. E, F) Optical microscope enlargements of the pattern.

film is then rinsed in toluene, leaving a patterned film behind with dimensions on the order of 1 mm shown in Figure 8C. After drying, the film was immersed in electrolyte and oxidized at 0.35 V, to bleach the patterned areas shown in Figure 8D. As mentioned previously, this photolithographic patterning was performed under standard laboratory conditions and, as expected, light crosslinking of the masked areas occurred. We expect that a higher contrast and finer detail can be achieved under rigorous lithographic conditions such as filtered light and controlled temperature in a cleanroom setting as is used for most photolithographic printing. It is understood that this is a first demonstration of this concept in regards to electrochromic conjugated polymers and that further optimization of processing and patterning are needed, but are beyond the scope of this paper.

Additionally, as with other polymer and organic electronic devices, such as organic photovoltaics (OPVs), organic light emitting diodes (OLEDs) and light emitting electrochemical cells (LEECs), most electrochromic devices consist of several successively deposited organic layers, with many of those

layers soluble in common solvents. By employing orthogonal processing methods, subsequent layers are processed (and the solvents used) without dissolving underlying layers. Several strategies have been explored within the area of OPVs and PLEDs,<sup>[22,43]</sup> that rely on a post-processing step where the coated layer is made insoluble in the next processing solvent. Ultimately this would enable the fabrication of devices from the bottom-up, a further step towards roll-to-roll processing. To that end, the copolymers presented here show promise where both the 30 and 60% copolymer are rendered insoluble in toluene after crosslinking suggesting they can additionally be ideal candidates for large area orthogonal coating.

## 4. Conclusion

In this report, we have presented a conjugated electroactive copolymer based on an alkoxy-substituted ProDOT and an acrylate-substituted ProDOT where the relative amount of monomer unit containing acrylate functionality relative to alkoxy was varied. This material is unique in that it allows solution processability of an electrochromic material from common organic solvents, followed by photo-crosslinking to render the film insoluble, while maintaining electrochemical, spectroscopic, and colorimetric properties. We have also shown the utility of such materials for printing and patterning by utilizing photolithographic methods whereby we created a patterned surface with millimeter-sized dimensions as a first demonstration. This opens the way for printing and patterning of fully solution processed and roll-to-roll coated conjugated electrochromic polymers for patterned displays as desired for applications such as e-readers, smart-cards, and information displays.

## 5. Experimental Section

**Instrumentation:**  $^1\text{H}$  and  $^{13}\text{C}$  NMR spectra were recorded on a Gemini 300 FT-NMR. IR spectroscopy was performed on an IRAffinity-1 from Shimadzu. The IR spectra were obtained using either Attenuated Total Reflectance (ATR) technique on the pure solids or transmission IR on polymer films spin-cast onto KBr pellets. Gel-permeation chromatography (GPC) was performed at 35 °C in THF to determine molecular weight(s). A combination of a Waters HPLC pump 1515, UV-vis Detector 2487, and a Refractive Index Detector 2414 were used. A Waters column (4.6 mm  $\times$  300 mm; Styragel HR 5E) and polystyrene standards from Fluka were used. The polymer solution (1 mg mL<sup>-1</sup> in THF) was prepared and filtered through a Mini-UniPrep PTFE vial with a 0.45  $\mu\text{m}$  filter. 20  $\mu\text{L}$  of each polymer solution was injected and molecular weights were calculated using Waters Breeze II software. Electrochemical analysis was performed using a Princeton Applied Research (PAR) model 273A Potentiostat/Galvanostat. Absorption profiles and spectroelectrochemical measurements were carried out on a Cary 5000 model UV-Vis-NIR from Agilent. Colorimetry studies were performed with a Konica Minolta CS-100 Chromameter.

**Crosslinking:** The polymer films were crosslinked using a Rayonet RPR-100 Photoreactor equipped with RPR-3500 lamps. The total irradiance was measured to 12 mW cm<sup>-2</sup> using a Thorlabs PM100 and individual wavelengths were measured using a Newport Optical Power Meter 1830C employing a 818-UV detector (SN2009). The irradiance at 350 nm was determined to be 0.7 mW cm<sup>-2</sup>.

**Film Formation:** For solubility studies, films of the various copolymers were spin-coated from 20 mg mL<sup>-1</sup> solutions of toluene or CHCl<sub>3</sub>. In addition, films subject to irradiation contained 6 mg mL<sup>-1</sup> AIBN and



~42 mg mL<sup>-1</sup> ethyleneglycoldimethacrylate (EGDMA). Films were cast onto ITO-coated float glass (1" × 1"; Delta Technologies, R<sub>s</sub> < 20 Ω/sq.) at an angular velocity of 800 rpm using a Laurell WS-400-6NPP spin-coater. For cyclic voltammetry, films were drop-cast onto a Pt-button electrode from a 0.5 mg mL<sup>-1</sup> toluene solution and allowed to evaporate leaving a thin film. Irradiated films contained 0.25 mg mL<sup>-1</sup> AIBN and ~2.1 mg mL<sup>-1</sup> EGDMA. For spectroelectrochemical measurements and direct photopatterning, thin films were spray-cast from a 2 mg/mL toluene solution using either a GREX genesis xg or Iwata-eclipse HP-BS airbrush, onto ITO-coated glass (Delta Technologies, CG-501N-10V, R<sub>s</sub> = 5–10 Ω). Irradiated films contained 1 mg/mL AIBN and ~6.3 mg mL<sup>-1</sup> EGDMA.

**Solubility Studies:** Thin films were spin cast onto ITO-coated glass as described above. The absorbance of the individual slides was measured using a Cary 5000 prior to irradiation. The samples were then irradiated for 0–600 s and the absorbance measured a second time after irradiation. The slides were then emerged into a stirring solution of toluene at room temperature for 60 s. After drying, the absorbance was measured a third time and the spectra plotted. In some instances the temperature of the toluene solution was raised to 100 °C.

**Spectroelectrochemical and Colorimetric Analysis:** Films were spray-cast, as described above, onto cuvette-size ITO-coated glass, and used as the working electrode (WE). The WE was submerged in a solution of 0.5 M tetrabutylammonium hexafluorophosphate (TBAPF<sub>6</sub>) in acetonitrile in a cuvette. A standard Ag/Ag<sup>+</sup> (10 mM AgNO<sub>3</sub> in 0.5 M TBAPF<sub>6</sub>/acetonitrile) was used as a reference electrode and a Pt flag was used as the counter electrode. The absorption spectrum was taken of the pristine film prior to any electrochemical switching. The films were electrochemically cycled between -0.1 and 0.4 V until a stable voltammetric response was obtained (typically 5 cycles), to allow incorporation of electrolyte into the polymer film. Potentiostatic experiments were then performed between 0 and 0.4 V and the absorbance spectra recorded at each potential. The same setup and procedure were used for colorimetric analysis. The ITO-coated glass was sprayed with the ECP so that the absorbance was between 0.79 and 0.84. After the initial break-in of the films, potentiostatic experiments were performed and the Y, x and y values measured using a Minolta Chromameter CS-100 colorimeter with a GraphicLite LiteGuard II standard D50 light source illuminating the sample from behind. The light source and the sample to be measured were placed in a color viewing booth. The interior of the light booth is coated with a standard gray neutral 8 (GTI Graphic Technology Inc.) matte latex enamel (equivalent to Munsell N8) to allow for accurate assessment of color of the sample during measurement. These values were subsequently used to calculate L\*a\*b\* values.

**Synthesis of (3,4-dihydro-2H-thieno[3,4-b][1,4] dioxepine-3,3-yl) bis(methylene)bis(2-methylacrylate):** Into a dry 250 mL round-bottomed flask was added anhydrous DMF (100 mL) in which ProDOT(CH<sub>2</sub>Br)<sub>2</sub> (5.0 g; 14.6 mmol) was dissolved. To this solution was added methacrylic acid (3.75 g; 43.8 mmol) and K<sub>2</sub>CO<sub>3</sub> (7.3 g; 52.8 mmol). A condenser was attached and the frothing solution was stirred under argon at 100 °C for 21 h, by which TLC (10% EtOAc in hexane) confirmed conversion of starting material. The solution was allowed to cool and water (150 mL) was added. The solution was extracted with DCM (3 × 100 mL), and the combined organic phases were washed twice with brine (2 × 100 mL). The organic phase was dried using MgSO<sub>4</sub> and concentrated in vacuo yielding a yellow-brownish oil. The crude compound was purified by dry column vacuum chromatography (DCVC) using EtOAc in hexane as the eluent (0 to 50%) in 50 mL fractions.<sup>[40]</sup> The pure compound appeared as a white solid with a blue hue. Yield 2.35 g (45%); mp 49–50 °C <sup>1</sup>H NMR (300 MHz, CDCl<sub>3</sub>): δ ppm 6.46 (s, 2H); 6.09 (s, 2H); 5.58 (s, 2H); 4.28 (s, 4H); 4.06 (s, 4H); 1.93 (s, 6H). <sup>13</sup>C NMR (300 MHz, DMSO-d<sub>6</sub>): 166.6, 149.5, 136.9, 127.9, 106.7, 72.6, 63.0, 46.2, 18.4; EIMS (m/z (%)): 352.1 (80) [M<sup>+</sup>], 353.1 (20) [M<sup>+</sup> + H], 83 (40); calc.: 352.098; found: 352.097.

**Synthesis of Poly(3,3-bis((2-ethylhexyl)oxy)methyl)-3,4-dihydro-2H-thieno[3,4-b][1,4]dioxepine-co(3,4-dihydro-2H-thieno[3,4-b][1,4]dioxepine-3,3-yl)bis(methylene)bis(2-methylacrylate):** Copolymers with various amounts of bis-methacrylate monomer were synthesized by varying

the amount of individual monomers in the reaction mixture. In a typical synthesis, a total of 2.8 mmol of monomers were added to a 50 mL round bottomed flask and dissolved in ethyl acetate (15 mL). The solution was bubbled thoroughly with argon for 60 min while stirred. The flask was placed in a water bath (20 °C). FeCl<sub>3</sub> (14 mmol, 2.2 g, 5 eq) was added to a small beaker of ethyl acetate (5 mL) and bubbled with argon for 1 min. The resulting yellow solution was added by syringe in one portion to the monomer solution resulting in an immediate color change to dark green/blue. The reaction flask was covered in foil and the water bath removed after 5 min. During the polymerization the reaction mixture was continuously bubbled with argon and stirred. The reaction was considered complete when the mixture was black and almost solid (around 3 h). The viscous dark mixture was transferred to a solution of MeOH (200 mL) and stirred for 60 min. Hereafter, it was filtered and the residue washed with MeOH until the filtrate became clear. The solid was dissolved in toluene (200 mL) and reduced with hydrazine (THF solution) until the resulting solution became bright purple (around 0.25 mL). The mixture was transferred to a separatory funnel and washed twice with water (2 × 200 mL), and the organic phase was concentrated in vacuo. The concentrate was precipitated in stirring MeOH (200 mL) and transferred to a cotton thimble. The precipitate was Soxhlet extracted with MeOH (24 h), hexanes (24 h) and CHCl<sub>3</sub> (24 h). The CHCl<sub>3</sub> fraction was concentrated in vacuo and reprecipitated in MeOH (200 mL). The solution was filtered and the solid dried under vacuum for 24 h yielding a magenta colored solid.

## Supporting Information

Supporting Information is available from the Wiley Online Library or from the author.

## Acknowledgements

J.R., A.D., and E.S. gratefully acknowledge support of BASF.

Received: October 15, 2012

Revised: December 29, 2012

Published online: March 6, 2013

- [1] P. M. S. Monk, R. J. Mortimer, D. R. Rosseinsky, *Electrochromism and Electrochromic Devices*, Cambridge University Press, Cambridge 2007.
- [2] R. J. Mortimer, A. L. Dyer, J. R. Reynolds, *Displays* **2006**, 27, 2–18.
- [3] C. G. Granqvist, *Sol. Energy Mater. Sol. Cells* **2000**, 60, 201–262.
- [4] C. G. Granqvist, *Sol. Energy Mater. Sol. Cells* **2012**, 99, 1–13.
- [5] F. C. Krebs, *Nat. Mater.* **2008**, 7, 766–767.
- [6] D. Mecerreyes, R. Marcilla, E. Ochoteco, H. Grande, J. A. Pomposo, R. Vergaz, J. M. Sánchez Pena, *Electrochim. Acta* **2004**, 49, 3555–3559.
- [7] A. A. Argun, P.-H. Aubert, B. C. Thompson, I. Schwendeman, C. L. Gaupp, J. Hwang, N. J. Pinto, D. B. Tanner, A. G. MacDiarmid, J. R. Reynolds, *Chem. Mater.* **2004**, 16, 4401–4412.
- [8] H. W. Heuer, R. Wehrmann, S. Kirchmeyer, *Adv. Funct. Mater.* **2002**, 12, 89–94.
- [9] B. D. Reeves, C. R. G. Grenier, A. A. Argun, A. Cirpan, T. D. McCarley, J. R. Reynolds, *Macromolecules* **2004**, 37, 7559–7569.
- [10] C. M. Amb, P. M. Beaujuge, J. R. Reynolds, *Adv. Mater.* **2010**, 22, 724–728.
- [11] A. L. Dyer, M. R. Craig, J. E. Babiarz, K. Kiyak, J. R. Reynolds, *Macromolecules* **2010**, 43, 4460–4467.
- [12] P. M. Beaujuge, S. Ellinger, J. R. Reynolds, *Nat. Mater.* **2008**, 7, 795–799.
- [13] G. Gunbas, L. Toppare, *Chem. Commun.* **2012**, 48, 1083–1101.

- [14] A. A. Argun, A. Cirpan, J. R. Reynolds, *Adv. Mater.* **2003**, *15*, 1338–1341.
- [15] J. Jensen, H. F. Dam, J. R. Reynolds, A. L. Dyer, F. C. Krebs, *J. Polym. Sci., Part B* **2012**, *50*, 536–545.
- [16] C. M. Amb, A. L. Dyer, J. R. Reynolds, *Chem. Mater.* **2011**, *23*, 397–415.
- [17] M. Dietrich, J. Heinze, G. Heywang, F. Jonas, *J. Electroanal. Chem.* **1994**, *369*, 89–92.
- [18] A. Kumar, D. M. Welsh, M. C. Morvant, F. Piroux, K. A. Abboud, J. R. Reynolds, *Chem. Mater.* **1998**, *10*, 896–902.
- [19] D. M. Welsh, A. Kumar, E. W. Meijer, J. R. Reynolds, *Adv. Mater.* **1999**, *11*, 1379–1382.
- [20] D. M. Welsh, L. J. Kloeppner, L. Madrigal, M. R. Pinto, B. C. Thompson, K. S. Schanze, K. A. Abboud, D. Powell, J. R. Reynolds, *Macromolecules* **2002**, *35*, 6517–6525.
- [21] A. Cirpan, A. A. Argun, C. R. G. Grenier, B. D. Reeves, J. R. Reynolds, *J. Mater. Chem.* **2003**, *13*, 2422–2428.
- [22] P. M. Beaujuge, C. M. Amb, J. R. Reynolds, *Adv. Mater.* **2010**, *22*, 5383–5387.
- [23] N. R. De Tacconi, K. Rajeshwar, R. O. Lezna, *Chem. Mater.* **2003**, *15*, 3046–3062.
- [24] Z. Nie, E. Kumacheva, *Nat. Mater.* **2008**, *7*, 277–290.
- [25] Y. Xu, F. Zhang, X. Feng, *Small* **2011**, *7*, 1338–1360.
- [26] S. Holdcroft, *Adv. Mater.* **2001**, *13*, 1753–1765.
- [27] J. Yu, M. Abley, C. Yang, S. Holdcroft, *Chem. Commun.* **1998**, *15*, 1503–1504.
- [28] M. S. A. Abdou, Z. W. Xie, A. M. Leung, S. Holdcroft, *Synth. Met.* **1992**, *52*, 159–170.
- [29] M. S. A. Abdou, S. Holdcroft, *Macromolecules* **1993**, *26*, 2954–2962.
- [30] J. Kim, J. You, E. Kim, *Macromolecules* **2010**, *43*, 2322–2327.
- [31] J. Kim, J. You, B. Kim, T. Park, E. Kim, *Adv. Mater.* **2011**, *23*, 4168–4173.
- [32] K. S. Schanze, T. S. Bergstedt, B. T. Hauser, *Adv. Mater.* **1996**, *8*, 531–534.
- [33] J. Lowe, S. Holdcroft, *Macromolecules* **1995**, *28*, 4608–4616.
- [34] A. Kumar, S.-Y. Jang, J. Padilla, T. F. Otero, G. A. Sotzing, *Polymer* **2008**, *49*, 3686–3692.
- [35] F. C. Krebs, *Sol. Energy Mater. Sol. Cells* **2009**, *93*, 394–412.
- [36] R. Søndergaard, M. Hösel, D. Angmo, T. T. Larsen-Olsen, F. C. Krebs, *Mater. Today* **2012**, *15*, 36–49.
- [37] H. F. Dam, F. C. Krebs, *Sol. Energy Mater. Sol. Cells* **2012**, *97*, 191–196.
- [38] F. C. Krebs, M. Jørgensen, K. Norrman, O. Hagemann, J. Alstrup, T. D. Nielsen, J. Fyenbo, K. Larsen, J. Kristensen, *Sol. Energy Mater. Sol. Cells* **2009**, *93*, 422–441.
- [39] H. Sirringhaus, T. Kawase, R. H. Friend, T. Shimoda, M. Inbasekaran, W. Wu, E. P. Woo, *Science* **2000**, *290*, 2123–2126.
- [40] D. S. Pedersen, C. Rosenbohm, *Synthesis* **2001**, *16*, 2431–2434.
- [41] K. Norrman, A. Ghanbari-Siahkali, N. B. Larsen, *Annu. Rep. Prog. Chem., Sect. C* **2005**, *101*, 174–201.
- [42] R. J. Mortimer, K. R. Graham, C. R. G. Grenier, J. R. Reynolds, *ACS Appl. Mater. Interfaces* **2009**, *1*, 2269–2276.
- [43] T. T. Larsen-Olsen, B. Andreasen, T. R. Andersen, A. P. L. Böttiger, E. Bundgaard, K. Norrman, J. W. Andreasen, M. Jørgensen, F. C. Krebs, *Sol. Energy Mater. Sol. Cells* **2012**, *97*, 22–27.